Multi-Element Synthetic Transmit Aperture in Medical Ultrasound Imaging

Ihor TROTS, Andrzej NOWICKI, Marcin LEWANDOWSKI,
Yuriy TASINKEVYCH

Institute of Fundamental Technological Research
Polish Academy of Sciences
Pawińskiego 5B, 02-106 Warszawa, Poland
e-mail: igortr@ippt.gov.pl

Synthetic aperture (SA) technique is a novel approach to present day commercial systems and has previously not been used in medical ultrasound imaging. The basic idea of SA is to combine information acquired simultaneously from all directions over a number of emissions and to reconstruct the full image from these data.

The paper presents the multi-element STA (MSTA) method for medical ultrasound imaging. The main difference with the STA approach is the use of a few elements in the transmit mode in contrast to a single element aperture. This allows increasing the system frame rate, decreasing the number of emissions, and provides the best compromise between the penetration depth and lateral resolution. Besides, a modified MSTA is proposed with a corresponding RF signal correction in the receive mode, which accounts for the element directivity property.

In the experiments a 32-element linear transducer array with 0.48 mm inter-element spacing and a burst pulse of 100 ns duration were used. Two elements wide transmission aperture was used to generate an ultrasound wave covering the full image region. The comparison of 2D ultrasound images of a tissue mimicking phantom obtained using the STA and MSTA methods is presented to demonstrate the benefits of the second one.

Keywords: ultrasound imaging, synthetic aperture, beamforming.

1. Introduction

The ultrasound imaging has become much more prevalent than other medical imaging techniques since it is more accessible, less expensive, safer, simpler to use, and produces real-time images. However, to provide an accurate clinical interpretation the highest possible image quality is required. The most commonly

used image quality measures are spatial resolution, image contrast and frame rate. The spatial resolution of the ultrasound image can be improved by using several transmit beams during the interrogation of each sector, each of which is focused at a different depth. It is done in modern ultrasound imaging systems at the cost of a decrease of the frame rate, proportionally to the number of transmit foci (HOLM, YAO, 1999). An alternative way to obtain an appropriate spatial resolution, without the decrease of the frame rate, is to use the synthetic aperture technique.

Synthetic aperture originates from radars and sonars and has previously not been used in the ultrasound medical imaging. The basic idea of SA is to gather information acquired simultaneously by small transmit-receive apertures placed in different positions and then to reconstruct the full image from the collected data. In the simplest case a single element transmits an unfocused wave and then it is switched to receive the backscattered signal which yields a low resolution image line. Combing the data obtained from a large number of emissions enables one to obtain a high resolution image.

There are several methods to form a synthetic aperture for ultrasonic imaging. The described above synthetic aperture focusing technique (SAFT) is the simplest one. It reduces the system complexity but is characterized by low signal-to-noise ratio and penetration depth. Multi-element synthetic aperture focusing (MSAF) is an alternative to SAFT. A group of elements transmits the unfocused wave-field and receives signals simultaneously. The acoustic power and the signal-to-noise ratio (SNR) are increased as compared to the SAFT. Synthetic transmit aperture (STA) is alternate to conventional phased array. At each time a single array element transmits an ultrasound pulse and all elements receive the echo signals (TROTS *et al.*, 2009). The advantage of this approach is that a full dynamic focusing can be realized in both transmit and receive modes, giving the highest image quality.

The main objective of this work is to implement the MSTA method in ultrasound imaging where only a few elements transmit unfocused wave-field and all array elements receive the echo signals. The main goal of the method is the increase of the system frame rate (by decreasing the number of emissions) and penetration depth. The latter is due to the increase of the transmitted energy which improves the SNR and, as a result, the ultrasound image contrast.

The paper is organized as follows. In the next section the MSTA algorithm is discussed. In Sec. 3 the RF signal corrections are introduced into MSTA accounting for the element directivity in the receive mode. This section strongly relies on the paper (TASINKEVYCH *et al.*, 2010) where a similar modification for the STA algorithm is discussed. In Sec. 4 the results of numerical computations are shown. The phantom data are simulated by means of the Field II program for Matlab®. In Sec. 5 the experimental setup is briefly discussed and, finally, in Sec. 6 some experimental results are given.

2. Multi-element synthetic transmit aperture

The main advantage of the proposed MSTA algorithm is the improvement of the lateral resolution and visualization depth of the resulting image. The former is known to be strongly related to the array length. Practically, it is not too difficult to build a large transmit aperture, but it is a very complicated task to realize a large receive aperture. In the proposed MSTA algorithm the transmit subaperture consists of a small number of elements, whereas all array elements receive the echo signals independently and the resulting RF echoes are stored in memory. The high resolution image is synthesized by coherent summing of all received echoes upon completion of the data acquisition cycle. On the other hand, the frame rate is increased in the MSTA due to the decrease of the total number of emissions, and this speeds up the data acquisition process.

A simple diagram explaining the MSTA algorithm is shown in Fig. 1. Let us consider an N element aperture. Each time Ns elements are used to transmit an unfocused wave, and all the elements receive the backscattered signal independently. In the successive emission the next Ns elements are used as shown in Fig. 1. In the considered MSTA algorithm the transmit subaperture is shifted by the number of elements Ns between consecutive transmissions. Thus, for N-element aperture, $M \times N$ data recordings are required for the image reconstruction, where $M = N/Ns$ is the number of emissions, $M \ll N$.
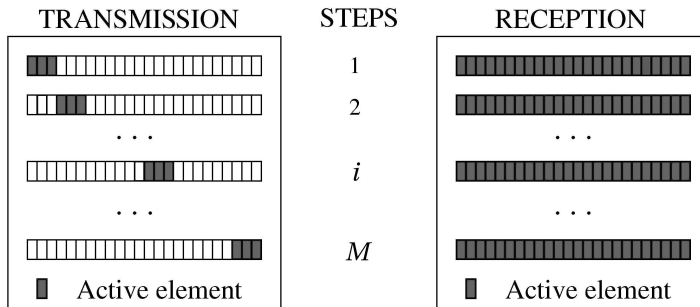

Fig. 1. Transmitting and receiving in MSTA method.

Thus, each subaperture transmits an unfocused beam and emulates a wider single element aperture.

In Fig. 2 the geometry of the transmission and reception for the MSTA system is illustrated, where (r, θ) is the current focusing point of the resulting image.

When a short pulse is transmitted by m-th transmit subaperture, where $m = 1, \ldots, M$, and the echo signal is received by element n, as shown in Fig. 2, a round-trip delay is

$$\tau_{m,n} = \tau_m + \tau_n, \tag{1}$$

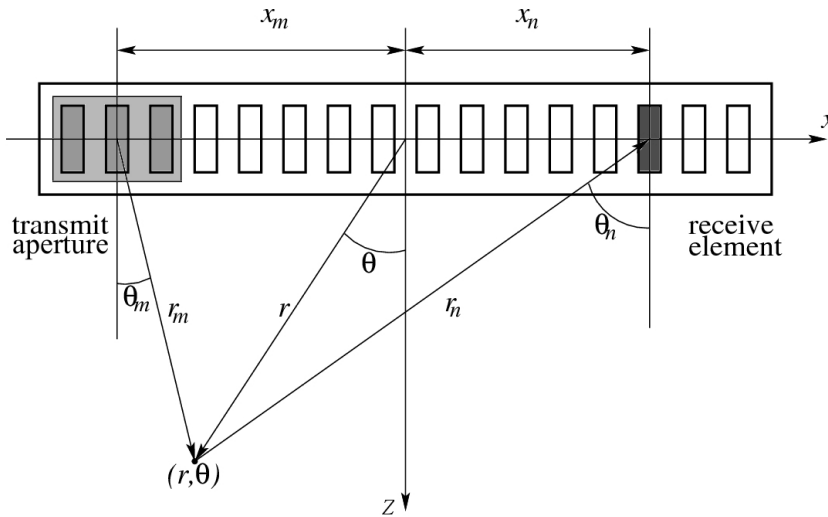where (m, n) is a transmit and receive element combination, $n = 1, \ldots, N$, $m = 1, \ldots, M$.

Fig. 2. Geometric relation between the transmit and receive element combination and the focal point.

The delays for m-th and n-th elements are

$$\tau_m = \frac{1}{c} \left(r - \sqrt{x_m^2 + r^2 - 2x_m r \sin \theta} \right),$$

$$\tau_n = \frac{1}{c} \left(r - \sqrt{x_n^2 + r^2 - 2x_n r \sin \theta} \right), \tag{2}$$

where x_m, x_n are the positions of the centre of the transmit subaperture and receive element, respectively; r is the distance between the synthetic aperture centre and the point (r, θ). For an N-element array and each point in the resulting image, the A-scan signal can be expressed as follows:

$$A_{\text{STA}}(r, \theta) = \sum_{m=1}^{M} \sum_{n=1}^{N} y_{m,n} \left(\frac{2r}{c} - \tau_{m,n} \right), \tag{3}$$

where $y_{m,n}(t)$ is the echo signal and $\tau_{m,n}$ is the beamforming delay for the (m,n) transmit-receive pair given in Eq. (1). The first and second summations correspond to the transmit and receive beamforming, respectively.

3. Element directivity diagram influence

In the described above beamforming methods for each point in the resulting image every combination of transmit-receive subaperture pairs contributes according to the round-trip propagation time only. The angular dependence is not taken into account. But, when the width of the array element is comparable to the wavelength corresponding to the nominal frequency of the emitted signal, the

point-like source model becomes inaccurate. The element directivity influences the partial contribution to the resulting signal $A(r, \theta)$ in Eq. (3) depending on the mutual position of the imaging point and transmit-receive subapertures. Here, a similar modification is applied for the MSTA imaging algorithm, as it was developed and described in (TASINKEVYCH *et al.*, 2010) for the case of STA (a single element is used in the transmit mode). In this case, however, the corresponding RF echoes' corrections are applied only in the receive mode:

$$A_{\text{STA}}(r, \theta) = \sum_{m=1}^{M} \sum_{n=1}^{N} f(\theta_n) y_{m,\,n} \left(\frac{2r}{c} - \tau_{m,\,n} \right). \tag{4}$$

where $\theta_n(r, \theta)$ is the corresponding observation angle for the n-th receive element and imaging point (r, θ) (see Fig. 2). Thus, the modification of MSTA is expressed by the weighted summation of properly delayed RF signals (like in the case of the conventional algorithm). The corresponding weights $f(\theta_n)$ are calculated by means of the single element directivity function as it was proposed for the STA algorithm in the above-cited work. The directivity function $f(\theta)$ can be calculated in the far-field approximation for a single element of the array transducer in an analogous manner as in (SELFRIDGE *et al.*, 1980):

$$f(\theta) = \frac{\sin(\pi d / \lambda \sin \theta)}{\pi d / \lambda \sin \theta} \cos \theta, \tag{5}$$

where d is the element width and λ is the wavelength. Some examples of the directivity function evaluated for different values of the ratio d/λ are shown in Fig. 3. Note that the values of d/λ correspond to the case where the element width $d = 0.75P$, P – the pitch, and P is 0.5, 1, or 1.5 of the λ, respectively. The above result applies to a narrow strip transducer with a time harmonic
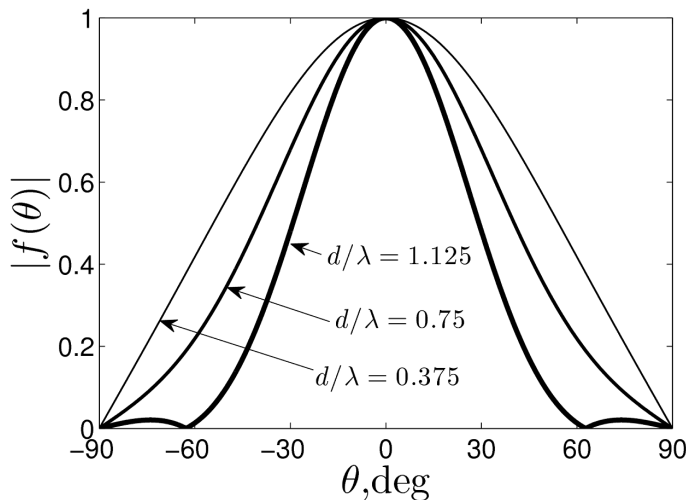

Fig. 3. Directivity function for different values of d/λ.

uniform pressure distribution along its width. Equation (5) is applied in the numerical results presented in the next section. It should be noted that we use the angular response $f(\theta)$ in Eq. (4) evaluated from Eq. (5) for some fixed value of λ, which corresponds to the nominal frequency of the transmitted signal. The far-field approximation is admissible for the case of the synthetic focusing algorithm discussed here. For the typical examples considered in the next section, the ratio $d/\lambda = 1.125$ is assumed, and the corresponding element directivity function is depicted in Fig. 3. The far-field limit $r_{\min} \approx 2d^2/\lambda$ (MICHISHITA *et al.,* 2000) is 2.5λ. This requirement is met in the considered numerical experiments.

4. Computer simulation

Simulation is a fundamental way of testing a developed method. This is done to confirm or reject a hypothesis in a controlled environment. Since it is possible to control all parameters in a simulation, one can set up a simple model and then gradually transform it into something more similar to reality. Once this is done, one can continue with measurements and confirm or reject the simulations for a real setup, in vivo or on a phantom.

The numerical results presented in Fig. 4 were performed for a 48-element linear transducer array excited by one sine cycle burst pulse at a nominal frequency of 5 MHz. The element pitch $P = 1.5\lambda$ and the element width $w = 0.75P$, where λ corresponds to the nominal frequency of the burst pulse. The MSTA algorithm is employed with 2 and 4 element transmit subapertures. The corresponding aperture shift between subsequent emissions is $2P$ and $4P$. The wire phantom was simulated by Field II program (JENSEN, 1999). Thin wires are spaced equidistantly with intervals of 6λ in the lateral and axial directions.
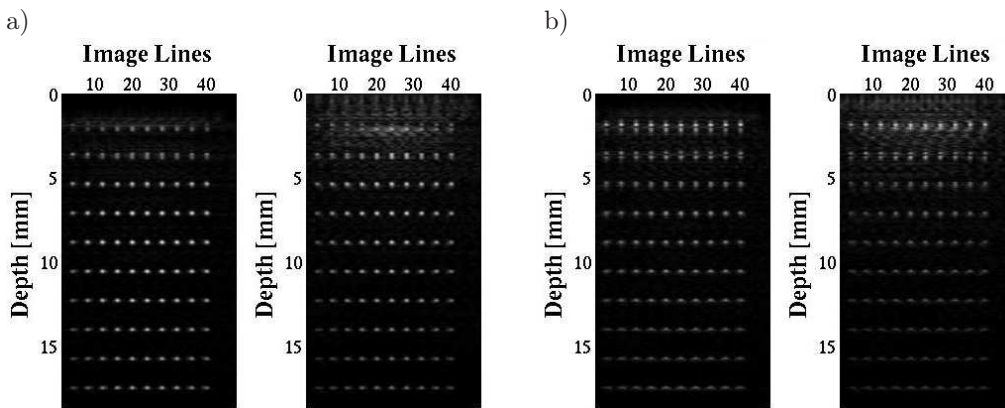

Fig. 4. Simulation of wire phantom for 48-element linear array: a) 2-element transmit subaperture and b) 4-element transmit subaperture; left subplots – with RF echoes correction (modified MSTA), right subplot – conventional MSTA. The magnitude of the scattered field in a linear scale is shown.

From Fig. 4 it is clearly observable that the artefacts around the scatterers near the transducer aperture, which are appreciable in the case of the conventional MSTA algorithm, are substantially suppressed in the case of the modified algorithm.

In Fig. 5 the 2D ultrasound images of a phantom obtained by computer simulation for the same transducer as in the previous example are shown. In the case of the MSTA method every subaperture consists of two elements and transmits an unfocused ultrasound wave. The phantom medium attenuation is 0.5 dB/[MHz×cm] and consists of collections of point targets spaced by 4 pitches apart laterally and 5 mm apart axially.
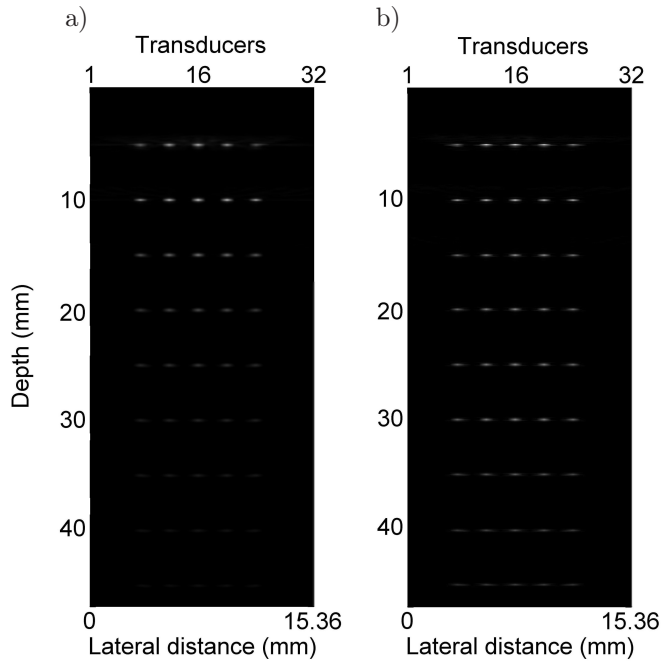

Fig. 5. Simulation of a wire phantom with point targets for the STA (left)
and MSTA (right) methods.

It can be easily seen that the penetration depth increases in the case of the MSTA method. For the objective comparison of the resolution the axial cross-sections of the centre line and lateral cross-sections at depths 10 mm and 20 mm are shown in Fig. 6. Note that in Fig. 6b the normalization is performed with respect to the maximum values of the corresponding cross-sections at a different depth, while in Fig. 6a the normalization is performed with respect to the maximum values of each line.

Figure 6 shows that the transmitted energy grows in the case of the MSTA method and the penetration depth increases, while the lateral resolution is comparable in both cases.
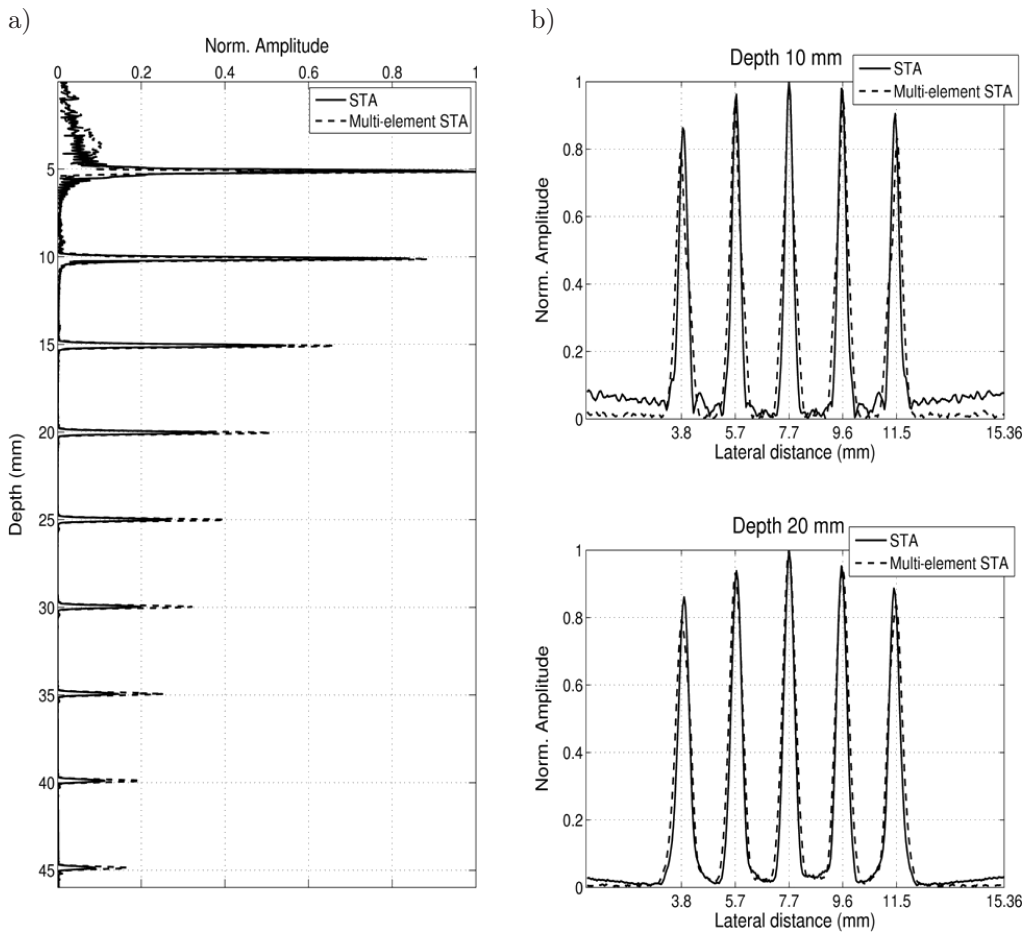
a)

b)

Fig. 6. Comparison of the cross-sections between the STA and MSTA methods: a) axial cross-section of the centre line; b) lateral cross-section at depths 10 mm (top) and 20 mm (bottom).

The MSTA imaging method represents the best solution in improving the penetration depth and maintaining the lateral resolution.

5. Ultrasound imaging system

A simplified ultrasound imaging system is shown in Fig. 7.

The transducer transmits pulses of the ultrasound waves and receives reflected echo signals. Echoson SG3 enables full control of selected 32 consecutive transducers of a linear array. Parameters of transmission and reception are programmable from a PC using a serial port (RS-232). Using a SG3 one can switch on arbitrary transmit and receive channels in the selected 32 channels aperture. The second block, i.e. A/D converter, extracts the RF data, acquires it and sends to the PC.
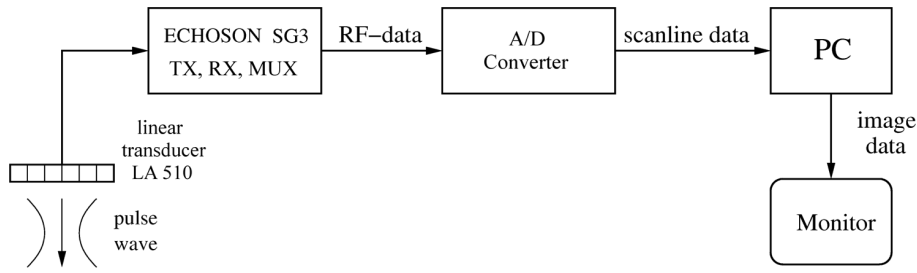
Fig. 7. Block diagram of an ultrasound imaging system.

Next, the collected digital data are processed offline and displayed on the monitor. All post-processing and display is done on the computer using Matlab. The processing creates 2D ultrasound imaging focused in every point of the image.

The system allows performing a simulated multichannel acquisition for synthetic aperture imaging. Using a single channel digitizer and switching receiving transducers the system is capable of gathering RF data for up to 32 lines. Repeating this procedure for each transmitted M subapertures of the N-element transducer the $M \times N$ data recordings needed for the image reconstruction that are the input to the MSTA algorithm are obtained.

Synthetic aperture image reconstruction requires considerable amount of data storage and processing power. In synthetic aperture processing all scan lines (full image) are created in each and every firing, whereas in the standard beamforming only a single line is created. The amount of raw RF data needed in the MSTA imaging for reconstruction of a single image is proportional to $D_{\mathrm{RF}} \cdot M \cdot N$, and the number of delay-and-sum operations is $D_{\mathrm{RF}} \cdot M \cdot N^2$, where D_{RF} is the number of samples in a single RF line. For a 32 element linear array and 2 elements in subaperture ($M = 16$) with 15 cm penetration ($D_{\mathrm{RF}} = 8000$ at 40 MHz sampling frequency) the storage requirements are about $4.1 \cdot 10^6$ samples, yielding approximately $131 \cdot 10^6$ delay-and-sum operations. This is twice lower than in the case of the STA method.

6. Experimental results and discussion

A 32-element linear transducer array with 0.48 mm inter-element spacing and a burst pulse with time duration 100 ns (a half-cycle at the nominal frequency 5 MHz) were used in the experiments. The inter-element space is about 1.5λ. All the elements were used for both transmitting and receiving. The comparison of the STA and MSTA methods was performed. In the case of the STA method one single element in the transducer transmitting aperture was used to generate an ultrasound wave covering the full image region. In the case of the MSTA method a two element transmit subaperture was implemented. This gives a total of 16×32 RF-lines in the case of the 2-element transmit subaperture, or 8×32 in the case of the 4-element one (32×32 in the case of the STA method). The RF echo sig-

nals were sampled independently at 50 MHz and processed by the corresponding MSTA and STA algorithms.

A tissue mimicking phantom model 525 Danish Phantom Design with attenuation of background material 0.5 dB/[MHz×cm] was used in the experiments. It consists of several nylon filaments' twists, 0.1 mm in diameter, positioned every 1 cm axially. This phantom allows examining the axial and lateral resolutions at various depths in the ultrasound image.

In Fig. 8 the received RF echo signals for the STA and MSTA methods, which were digitized and stored in the PC, are shown.
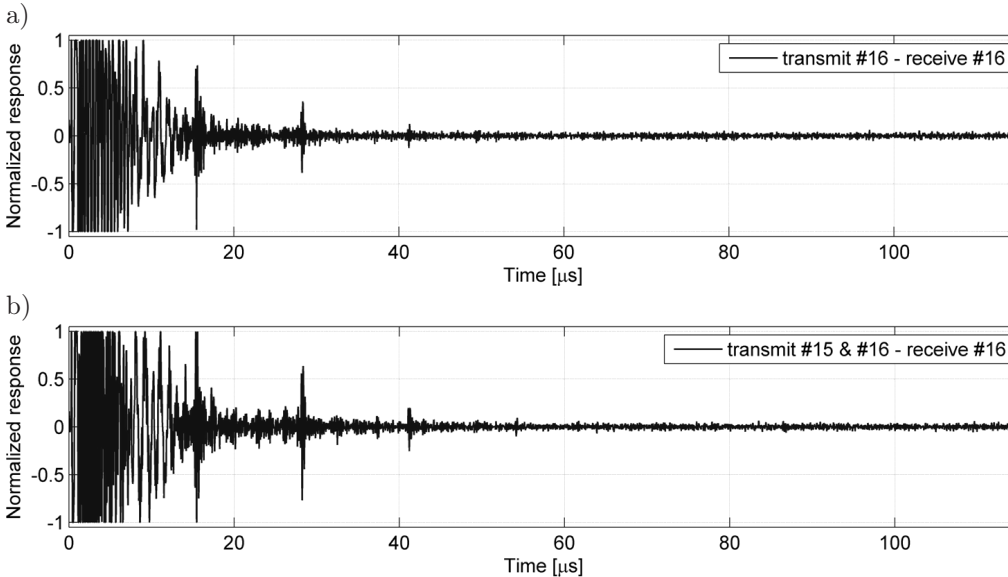
a)

b)

Fig. 8. The recorded echo signals: a) the STA method: element #16 is transmitting – element #16 is receiving, b) the MSTA method: elements #15 and #16 transmitting – #16 receiving.

It can be easily seen that the amplitude of the echo signals in the case of the MSTA method is approximately twice as high.

The comparison of the 2D ultrasonic images of a tissue phantom obtained by the conventional STA and MSTA methods is shown in Fig. 9.

The obtained 2D ultrasonic images clearly demonstrate the advantage of the MSTA method. With the enlargement of the transmit subaperture the acoustical power increases yielding a higher SNR, which leads to an increase in the penetration depth maintaining both the axial and lateral resolutions. The latter strongly depends on the transducer acoustic field and is discussed in (NOWICKI *et al.*, 2007).

In order to compare quantitatively the SNR gain the central RF-lines of the 2D ultrasound images shown in Fig. 9 are depicted in Fig. 10 and the SNR is calculated. For this purpose the noise level which appeared straight after the signal was chosen.
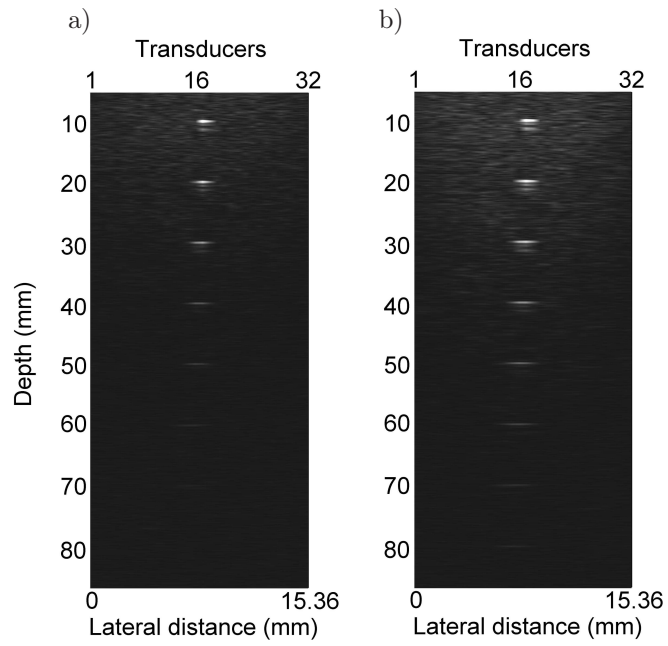
a)

Transducers

b)

Transducers

Fig. 9. 2D ultrasound images of a tissue mimicking phantom: a) using the STA method;
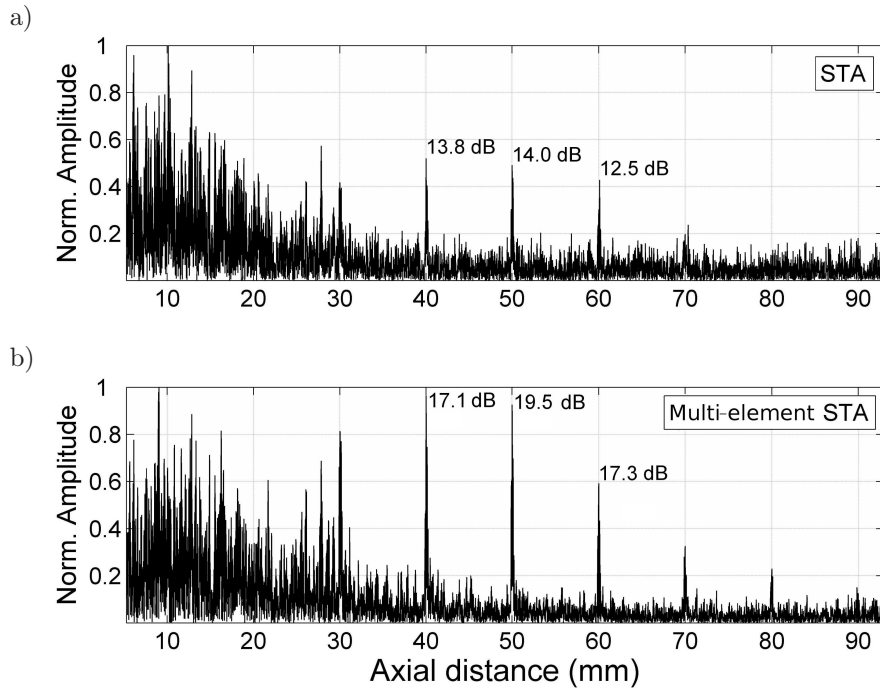b) using the MSTA method with a 2-element transmit subaperture.

a)

b)

Fig. 10. The RF-lines of the tissue mimicking phantom: a) using the STA method; b) using
the MSTA method with a 2-element transmit subaperture.

Figure 10 shows that increasing the transmit subaperture by one element improves SNR by about 5 dB, which in turn leads to improvement of the penetration depth and the contrast of the synthesized image.

In Fig. 11 the comparison of the original and modified MSTA algorithms (Eqs. (3) and (4), respectively) is illustrated. The image in Fig. 11a corresponds to the 2-element transmit subaperture, while in Fig. 11b shows the 4-element one. The shifts between subsequent emissions are $2P$ and $4P$, respectively.
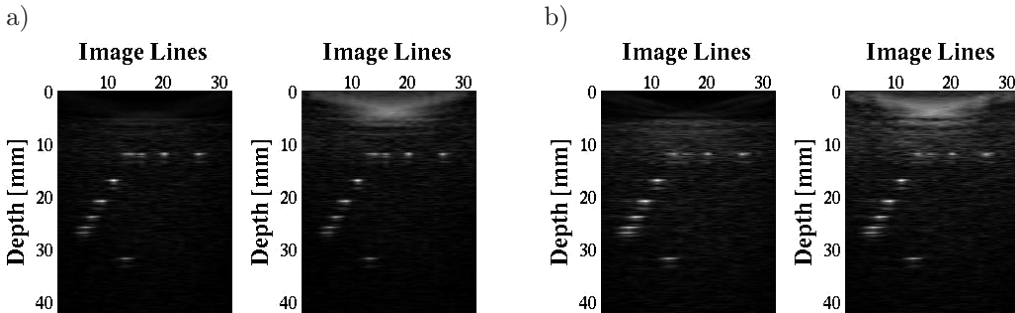
a)

b)

Fig. 11. 2D ultrasound images of the tissue mimicking phantom for a 32-element linear array using experimental data: a) 2-element transmit subaperture and b) 4-element transmit subaperture; left subplots – with RF echoes correction (modified MSTA), right subplots – conventional MSTA.

From Fig. 11 it is clearly observable that the artefacts around the scatterers located in the vicinity of the transducer are deprecated significantly in the case of the modified MSTA as compared to the one without the RF echoes correction.

7. Conclusion

The work concerns the development and investigation of the multi-element STA (MSTA) imaging algorithm where a few elements are used to transmit a pulse but all array elements receive the echo signals. This approach allows increasing the system frame rate and penetration depth maintaining the resolution of images. It is shown that even for a two element transmit subaperture the SNR can be improved by approximately 5 dB maintaining the same imaging resolution as in the case of the conventional STA. This, in its turn, allows improving the penetration depth and makes the ultrasound image more contrast.

The paper presents an example of how medical synthetic aperture ultrasound imaging can be acquired and processed. The MSTA method was investigated by both simulation and experimentally. The tissue mimicking phantom was used to test the image quality.

The modified MSTA algorithm is presented as well. It is based on the array element angular directivity function implementation into the conventional MSTA method, similar to an earlier case with the standard STA algorithm. The modified

MSTA is implemented in the form of a weighed summation of properly delayed RF echoes. However, in contrast to the STA algorithm, in this case the weighing is done only in the receive mode. The results of the numerical calculations using simulated data, as well as experimentally obtained ones for different phantoms, have shown a distinguishable improvement of the imaging quality of the scatterers situated in the vicinity of the transducer aperture. The hazy blurring artefacts, observable in the case of the conventional MSTA algorithm, are substantially suppressed in the case of the modified MSTA.

The MSTA method can be applied in a standard ultrasound scanner. An introduction of this method in medical ultrasound would increase the efficiency and quality of the ultrasound diagnostic.

Acknowledgments

Preliminary results of this study were presented at the Open Seminar on Acoustics, Gliwice, September 20–24, 2010.

References

1. Jensen J.A. (1999), *Linear description of ultrasound imaging systems*, Notes for the International Summer School on Advanced Ultrasound Imaging, Technical University of Denmark, July 5–9.

2. Holm S., Yao H. (1999), *Method and apparatus for synthetic transmit aperture imaging*, US patent No 5.951.479, September 14.

3. Michishita K., Sakagami K., Morimotgo M., Svensson U.P. (2000), *Sound radiation from an unbaffled elastic plate strip of infinite length*, Applied Acoustics, **61**, 1, 45–63.

4. Nowicki A., Klimonda Z., Lewandowski M., Litniewski J., Lewin P.A., Trots I. (2007), *Direct and post-compressed sound fields for different coded excitation*, Acoustical Imaging, **28**, 399–407.

5. Selfridge A.R., Kino G.S., Khuri–Yakub B.T. (1980), *A theory for the radiation pattern of a narrow-strip acoustic transducer*, Appl. Phys. Lett., **37**, 1, 35–36.

6. Tasinkevych Y., Nowicki A., Trots I. (2010), *Element directivity influence in the synthetic focusing algorithm for ultrasound imaging*, Proceedings of the 57th Open Seminar on Acoustics OSA 2010, pp. 197–200, September 2010, Gliwice, Poland, 2010.

7. Trots I., Nowicki A., Lewandowski M. (2009), *Synthetic transmit aperture in ultrasound imaging*, Archives of Acoustics, **34**, 4, 685–695.